Influence of Temperature and Operation Time on the Fatigue Strength and Microstructure of Welded Joints of A-387Gr.B Steel

5 authors, including:

Ivica Camagic
University of Pristina
57 PUBLICATIONS **128** CITATIONS

SEE PROFILE

Srdjan Jovic
University of Pristina
101 PUBLICATIONS **738** CITATIONS

SEE PROFILE

Zijah Burzic
Military Technical Institute, Belgrade
139 PUBLICATIONS **439** CITATIONS

SEE PROFILE

Some of the authors of this publication are also working on these related projects:

Multi-Criteria Optimization Method View project

dalibor petkovic View project

INFLUENCE OF TEMPERATURE AND OPERATION TIME ON THE FATIGUE STRENGTH AND MICROSTRUCTURE OF WELDED JOINTS OF A-387Gr.B STEEL

I. Čamagić,[1] **S. Jović,**[1,2] **S. Makragić,**[1] **P. Živković,**[1] **and Z. Burzić**[3]

The main aim of our paper is to analyze the influence of temperature and service time on the fracture resistance of welded joint constituents for new and exploited low-alloyed A-387Gr.B steel (Cr–Mo type) under the action of dynamic load and changes in the mechanical properties. The exploited parent metal, as a part of the reactor mantle, is in the damage repair stage, i.e., a part of its mantle is replaced with a new material. Wohler's curves were constructed, i.e., the fatigue strength as material resistance to crack initiation, was determined at the room and working temperatures. Testing of the welded joint and microstructural analyses of the parent metal, weld metal, and the heat-affected zones were carried out. Based on the testing results, the analysis of the fracture resistance, and the microstructural changes, represent the comparison of values obtained for the characteristic areas of the welded joint and the justification of the selected technology of welding.

Keywords: crack, low-alloyed steels, welded joints, fatigue strength, mechanical properties.

Introduction

A long-term period of operation of a pressure vessel – reactor (over 40 yr) causes certain damage to the reactor mantle. The occurrence of this damage demands a thorough inspection of the reactor structure itself, along with repairing of the damaged parts. Reactor repairs included the replacement of a part of the reactor mantle with a new material. The pressure vessel considered in the present work was made of low-alloy Cr–Mo A-387Gr.B steel in accordance with the ASTM standard with 0.8–1.15% Cr and 0.45–0.6% Mo. For the designed operating parameters ($p = 35$ bar and $t = 537°C$), the material is in the area where it is prone to the decarbonization of the surface in contact with hydrogen. As a consequence of surface decarbonization, the material strength may be reduced. The reactor represents a vertical pressure vessel with cylindrical mantle. Deep lids are welded on the top and bottom sides of the mantle of the same quality as the mantle itself. Inside the reactor, the most important process takes place in the stage of motor gasoline production and involves platforming in order to change the structure of hydrocarbon compounds and, thus, achieve a higher-octane rating. We tested new and exploited parent metal (PM), the components of welded joints [weld metal (WM) and heat affected zones (HAZ)], as well as the low-alloyed steel from which the reactor is made.

The exploited PM was made of A-387Gr.B steel with a thickness of 102 mm. The chemical compositions and mechanical properties (Table 1) of the exploited and new PM (according to the test documentation) are presented below. The chemical compositions of the exploited and new PM specimens (wt.%) were as follows:

[1] University of Pristina, Faculty of Technical Sciences, Kosovska Mitrovica, Serbia.

[2] Corresponding author; e-mail: srdjanjovic2016@hotmail.com.

[3] Military Technical Institute, Belgrade, Serbia.

Table 1
Mechanical Properties of the Exploited and New PM Specimens

Specimen	Yield stress, $R_{p0.2}$	Tensile strength, R_m	Elongation, A, %	Impact energy, J
	MPa			
E	320	450	34.0	155
N	325	495	35.0	165

Table 2
Mechanical Properties of Additional Materials

Additional material	Yield stress, $R_{p0.2}$	Tensile strength, R_m	Elongation, A, %	Impact energy, J at 20°C
	MPa			
LINCOLN Sl-19G	515	610	20	> 60
LINCOLN LNS-150	495	605	21	> 80

specimen E (C – 0.15, Si – 0.31, Mn – 0.56, P – 0.007, S – 0.006, Cr – 0.89, Mo – 0.47, and Cu – 0.027) and specimen N (C – 0.13, Si – 0.23, Mn – 0.46, P – 0.009, S – 0.006, Cr – 0.85, Mo – 0.51, and Cu – 0.035).

Welding of steel sheets made of the exploited and new PM was performed in two stages according to the requirements given in the welding procedure provided by a welding expert. These stages included: root weld of specimen E by using a coated LINCOLN S1 19G electrode (AWS: E8018-B2) and filling by arc welding under the powder protection; here, the wire (denoted by LINCOLN LNS-150) and the powder (denoted by LINCOLN P230) were used as additional materials.

The chemical compositions of the coated electrode LINCOLN S1-19G and the wire LINCOLN LNS-150 (according to the test documentation) are given below. The chemical compositions of the additional welding materials are as follows: LINCOLN S1-19G: C – 0.07, Si – 0.31, Mn – 0.62, P – 0.009, S – 0.010, Cr – 1.17, and Mo – 0.54; LINCOLN LNS-150: C – 0.10, Si – 0.14, Mn – 0.71, P – 0.010, S – 0.010, Cr – 1.12, and Mo – 0.48. Their mechanical properties, also according to the test documentation, are presented in Table 2.

A butt welded joint was made with a U-weld. The shape of the groove for welding preparation was chosen based on the sheet thickness, in accordance with the appropriate SRPS EN ISO 9692-1:2012 [2] and SRPS EN ISO 9692-2:2008 [3] standards.

Evaluation of the Fatigue Strength

Metal fatigue is defined as the process of cumulative damage under the action of variable loads, which manifests itself in the occurrence of cracks and fracture. Fatigue strength of welded joints is determined by testing
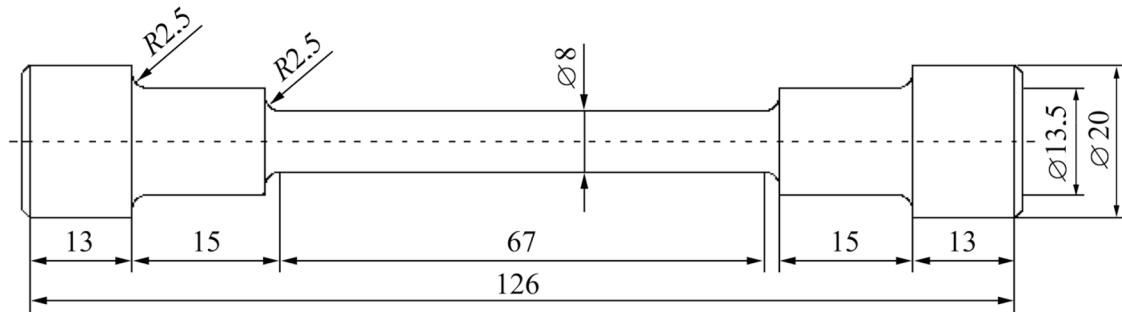
Fig. 1. Specimen for dynamic testing according to ASTM E466.

the specimens under variable loads that lead to the initiation of cracks or fracture. In the case of reactors, i.e., pressure vessels operating under increased pressure and temperature conditions, high-cycle fatigue tests are of particular importance. The strength of welded joints under variable loads observed in nonstationary operating modes of the reactors in the course of startups and shutdowns serves as an important characteristic for the evaluation of the integrity and remaining life. At the same time, it should be taken into account that a crack-like damage occurs after a large number of changes in the load under stresses much lower than the yield stress (high-cycle fatigue). Under loads whose levels are lower than yield stress, typical of high-cycle fatigue, it is a common practice to perform tests in the rigid mode.

High-cycle fatigue depends on the properties of constituents of the welded joint. The characteristics of high-cycle fatigue start significant changes only at temperatures above 400°C for steels used for pressure vessels and their welded joints.

Testing of the effects of temperature and exploitation duration on the behavior of the new PM, as well as on the behavior of butt welded joints subjected to variable load was performed to determine the points in the S–N-diagram (drawing of Wohler's curve) and fatigue strength (S_f) of the welding procedure. Moreover, the specimens were tested according to the ASTM E466, ASTM E467 and ASTM E468 standards [4–6]. The shape of the specimen tested under variable load is shown in Fig. 1.

Testing was carried out in a high-frequency pulsator. The values of the achieved frequency ranged between 115 and 165 Hz depending on the load and testing temperature. In order to fully evaluate the behavior of materials subjected to variable loads, while taking into account the dimension of the specimen, the most critical case of variable load was considered with the use of a variable load alternating between tension and pressure $(R = -1)$.

During this testing, it is a general rule to determine only the number of load changes until fracture under the load with a constant range, while the standard requires only the data about the magnitude of stresses for which crack initiation and fracture do not occur after a specific number of cycles (typically between 10^6 and 10^8 cycles). For steel materials, the ASTM E466 standard defines S_{strress}, S_f after 10^7 cycles.

The effect of exploitation duration and temperature on S_{strress}, S_f, i.e., the maximum dynamic stress under which there is no initiation of crack-like defects in shapes with smooth structures, is graphically shown in the form of Wohler's curves (S–N-diagrams) in Fig. 2a for specimens with butt welded joints and in Fig. 2b for specimens cut out from the new PM [1].

Testing of specimens of the PM was not performed because all specimens of welded joint cracked in the zone of the exploited PM and, hence, these tests provided the characteristics of the welded joint and PM.

In order to draw Wohler's curve and determine the fatigue strength, it is necessary to test the specimens for 6–7 different levels of loading.
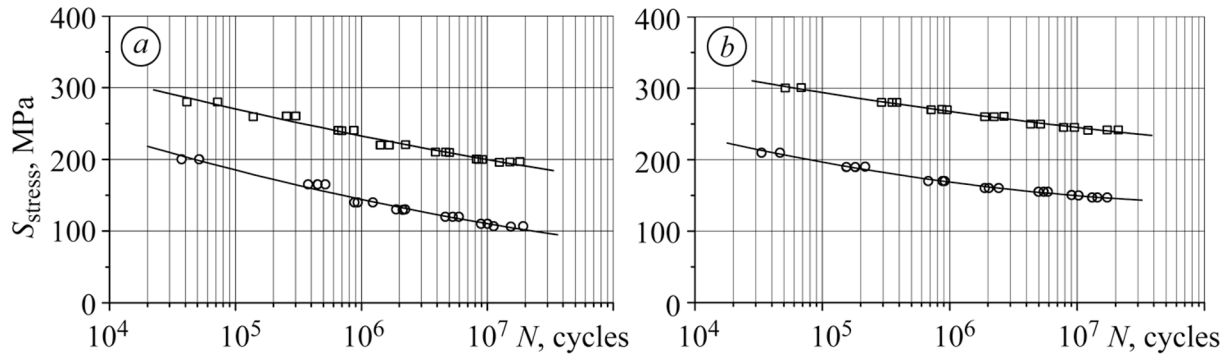
Fig. 2. S–N-diagram for the specimens cut out from the butt welded joint (a) and from the new PM (b) and tested at room and working temperatures: (□) 20°C; (○) 540°C.
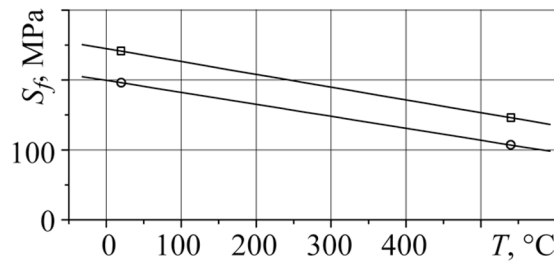
Fig. 3. Behavior of the S_f values for specimens cut out from the new PM and a butt welded joint depending on temperature: (□) new PM; (○) welded joint.

According to the ASTM E 466 standard, three specimens were tested for each load level, which made a total of 21 specimens. For this reason, the proposed tests are very cost-intensive and, hence, are justified only when the data are necessary for designing, first of all from the aspect of fatigue and fracture mechanics; in other words, when the parts subjected to long-term variable loads are designed as a part of the total designed structure life.

The effect of testing temperature on S_{strress}, S_f obtained by testing the specimens cut out from a butt welded joint and the new PM is shown in Fig. 3 [1].

Macro- and Microstructural Testing

For the successful application of A-387Gr.B steel and in order to obtain its maximal creep resistance, guaranteed mechanical properties are requested at higher temperatures, as well as the creep resistance at exploitation temperatures within a period that can be longer than 150,000 h. These properties are obtained with the proper thermal treatment providing the structure consisting of ferrite and bainite. Very fine carbides that start to sediment during this thermal treatment segregate on the grain boundary, as well as within the grain, which can be seen at high magnifications [7, 8].

Carbide precipitation, which begins during thermal treatment for the relaxation of residual stresses, continues in the course of operation at the exploitation temperatures and pressures [9, 14]. The appearance of these brittle phases can be ascertained by the data of metallographic analysis obtained under high magnification. This testing was conducted in order to evaluate the period of operation the parent metal and the components of welded

Fig. 4. Macrorecording of welded joint.
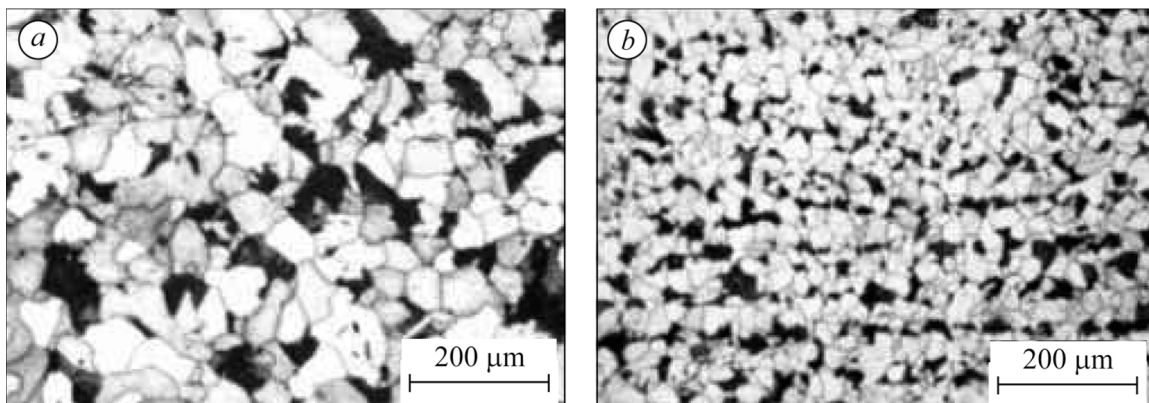
Fig. 5. Microstructures of the exploited PM (a) and new PM (b); ferrite-perlite structure.

joints depending on the variations of the microstructural properties. The macrorecording of a butt welded joint of the new PM and exploited PM is presented in Fig. 4 [1].

After etching of the butt welded joint, we can clearly distinguish the new and exploited parent metal; the heat affected zones on both sides, and the weld metal with well-marked groove filling zone.

Both parent metals show even structures that consist of bright polygonal ferrite crystals and transformed areas that can be analyzed under high magnifications. These transformed areas represent dark surfaces of perlite that looks like a compact dark microconstituent. The microstructure of the PM after operation for more than 40 yr is shown in Fig. 4 and the PM microstructure is shown in Fig. 5 [1]. The difference is in the grain size. A newly installed parent metal has a structure with grain size 5 according to the ASTM scale, while the exploited material has a structure with grain size 3 according to the ASTM scale.
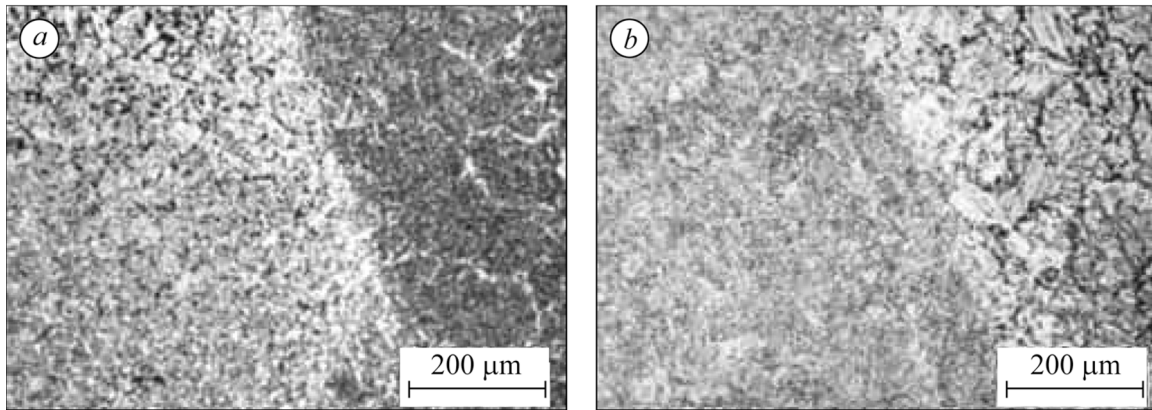
Fig. 6. HAZ microstructure for the used (a) and new PM (b).
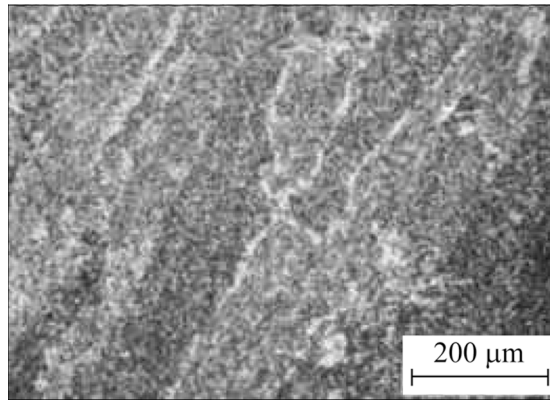
Fig. 7. WM microstructure; dendrite structure of the weld metal.

It is clear that, at a ×100 magnification, it is impossible to detect a noticeable difference between the degraded and new material, except in the grain size.
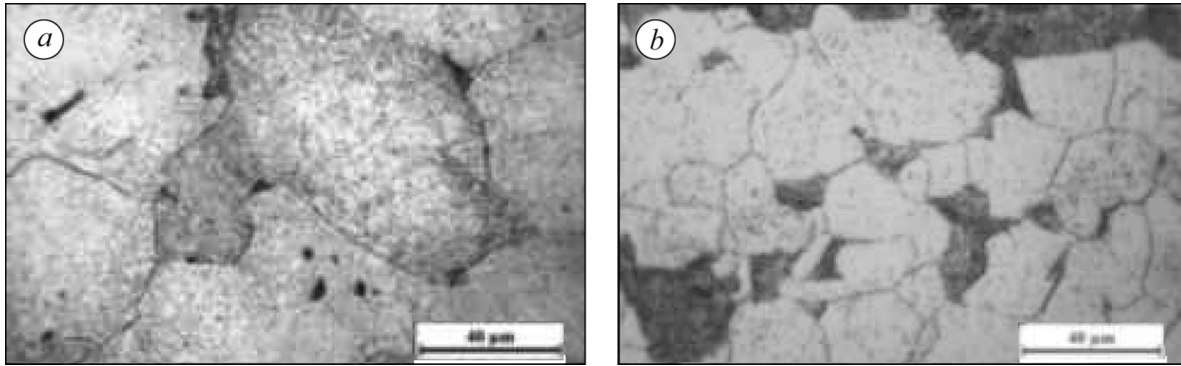
The microstructures of the HAZ on the degraded and new PM sides are shown in Fig. 6 [1]. They consist of ferrite, bainite and perlite. A bainite in the HAZ is formed as a consequence of a higher cooling rate of a part of the parent metal heated to the austenitizing temperature in the course of welding. A bainite level reduces the increase in the distance from the joint line.

A weld-metal structure with large dendrite created as a consequence of the foundry bath size and dimensions of the welded plates is shown in Fig. 7 [1].

Higher magnifications (×500 and more) enabled us to reveal the differences in the structural properties of the exploited and new PM. The period of operation of more than 40 yr affected the presence of carbides on the grain boundaries and within the grains. The amount of carbides in the new PM is much lower and the carbides are smaller (Fig. 8) [1].

CONCLUSIONS

The resistance of the material to crack initiation is determined as a result of fatigue-strength testing of materials. This is the maximum value of stress for which crack initiation does not occur for smooth specimens.

Fig. 8. Microstructures of the degraded PM (a) and new PM (b).

The higher the ratio of fatigue strength to yield stress, the better its resistance to crack initiation. By analyzing the results obtained as a result of high-cycle fatigue testing of smooth specimens for the purposes of plotting Wohler's curves and evaluation of the fatigue strength, it can be shown that the duration of exploitation has a predominant effect on the obtained values of fatigue strength. In case of testing of the specimens of welded joints made of the exploited PM at room temperature, the ratio of the fatigue strength to yield stress is 0.68, i.e. the obtained level of fatigue strength represents 68% of the yield stress. All specimens of welded joints broken in the course of the tests carried out under loads higher than the fatigue load suffered cracking either in the exploited PM or in the HAZ on the side of the exploited PM. The effect of testing temperature is such that an increase in temperature reduces the fatigue strength. In this case, the specimens of welded joint failed either in the exploited PM or in its HAZ. The crack initiation resistance for testing at 540°C decreases, i.e., the trend toward brittle fracture becomes more pronounced. The test results and their analysis justify the choice of welding technology for the purpose of replacing of a part of the reactor mantle.

REFERENCES

1. I. Čamagić, *Investigation of the Effects of Exploitation Conditions on the Structural Life and Integrity Assessment of Pressure Vessels for High Temperatures* (Doctoral-Degree Thesis, University of Pristina), Faculty of Technical Sciences with the Seat in Kosovska Mitrovica (2013).
2. *ISO 9692-1:2003. Welding and Allied Processes – Recommendations for Joint Preparation – Part 1: Manual Metal-Arc Welding, Gas-Shielded Metal-Arc Welding, Gas Welding,* TIG Welding and Beam Welding of Steels (2003).
3. *EN ISO 9692-2:1998. Welding and Allied Processes – Joint Preparation,* Part 2: *Submerged Arc Welding of Steels* (1998).
4. *ASTM. E466-07. Standard Practice for Conducting Force Controlled Constant Amplitude Axial Fatigue Tests of Metallic Materials,* ASTM Int., West Conshohocken, PA (2007).
5. *ASTM E467-89. Standard Practice for Verification of Constant Amplitude Dynamic Loads in an Axial Load Fatigue Testing Machine,* Annual Book of ASTM Standards (1989), Vol. 03.01, P. 577.
6. *ASTM E468-89. Standard Practice for Presentation of Constant Amplitude Fatigue Test Results for Metallic Materials,* Annual Book of ASTM Standards (1989), Vol. 03.01, P. 582.
7. Y. Kikuta, *Classification of Microstructures in Low-C, Low-Alloy Steel Weld Metal and Terminology,* Committee of Welding Metallurgy of the Lapan Welding Society (p. 15). Report No. IX-1281-83 (1983).
8. *Metals Handbook,* Vol. 6: Metalography, ASM Int. (1998), P. 1124.

9. R. C. Cochrane, *Weld Metal Microstructures: A State-of-the-Art Review*, International Institute of Welding (1982).

10. B. S. Kasatkin and O. N. Kozlovets, "Microctructure and low-alloy steel welded joints properties (Review)," *Paton Welding Journal C/C of Avtomaticheskaia Svarka*, No. 7, 1–11 (1989).

11. Z. Burzić, I. Čamagić, and A. Sedmak, "Fatigue strength of a low-alloyed steel welded joints," in: *The 3rd IIW South–East European Welding Congr. "Welding and Joining Technologies for a Sustainable Development and Environment," June 3–5, 2015, Timisoara, Romania*, Proc., 135–138 (2015); ISBN 978-606-554-955-5.

12. I. Čamagić, N. Vasić, S. Jović, Z. Burzić, and A. Sedmak, "Influence of temperature and exploitation time on tensile properties and microstructure of specific welded joint zones," in: *5th Internat. Congr. of Serbian Society of Mechanics, June 15–17, 2015, Arandjelovac, Serbia* (2015).

13. O. I. Balyts'kyi and I. F. Kostyuk, "Strength of welded joints of Cr–Mn steels with elevated content of nitrogen in hydrogen-containing media," *Fiz.-Khim. Mekh. Mater.*, **45**, No. 1, 88–96 (2009); **English translation:** *Mater. Sci.*, **45**, No. 1, 97–107 (2009).

14. A. I. Balitsky, I. F. Kostyuk, and O. A. Krokhmalny, "Physical-mechanical nonhomogeneity of welded joints of high-nitrogen Cr–Mn steels and their corrosion resistance," *Paton Welding J. C/C of Avtomaticheskaia Svarka*, No. 2, 26–29 (2003).